

Multiple instance learning on deep features for weakly supervised object detection with extreme domain shifts

Nicolas Gonthier^{a,b,*}, Saïd Ladjal^a, Yann Gousseau^a

^a*LTCI, Télécom Paris, Institut Polytechnique de Paris, 19 Place Marguerite Perey, 91120 Palaiseau, France*

^b*Université Paris-Saclay, 91190, Saint-Aubin, France*

Abstract

Weakly supervised object detection (WSOD) using only image-level annotations has attracted a growing attention over the past few years. Whereas such task is typically addressed with a domain-specific solution focused on natural images, we show that a simple multiple instance approach applied on pre-trained deep features yields excellent performances on non-photographic datasets, possibly including new classes. The approach does not include any fine-tuning or cross-domain learning and is therefore efficient and possibly applicable to arbitrary datasets and classes. We investigate several flavors of the proposed approach, some including multi-layers perceptron and polyhedral classifiers. Despite its simplicity, our method shows competitive results on a range of publicly available datasets, including paintings (People-Art, IconArt), watercolors, cliparts and comics and allows to quickly learn unseen visual categories.

Keywords: weakly supervised object detection, domain adaptation, non-photographic images, multiple instance learning

1. Introduction

The task of object detection has witnessed great progresses over the last few years, most notably through the development of clever and pragmatic combinations of region proposal methods and deep neural network architectures [1]. Nevertheless, the training of such architectures is well known to necessitate huge databases of manually annotated images. In the case of object detection, these annotations are extremely costly. It requires around one minute for a non expert to draw a bounding box around an object [2]. For more specialized datasets, such as artworks databases for instance, experts are likely to be reluctant to such annotations. The usual way to annotate such databases is to rely on specialized micro-tasks platforms such as Amazon Mechanical Turk.

*Corresponding author

Email address: nicolas.gonthier@telecom-paris.fr (Nicolas Gonthier)

This, by creating social exploitation and excessive precariousness, poses serious ethical concerns [3]. For these reasons, reducing the annotation stage is of great importance. In particular, many Weakly Supervised Object Detection (WSOD) methods have been developed [4, 5, 6] in order to train detection architectures using annotations only at image level, thus avoiding the precise localization of objects.

On the other hand, many different image modality exist for which object detection is desirable. Such modality include photographs taken in difficult conditions, as it is common in the case of autonomous driving [7], different imaging modality as in medical [8] or satellite imaging [9] or even hand created images such as artworks, clipart, etc. In such cases, available databases may be small and it is essential to be able to reuse information gathered on existing large photographic databases, a strategy known as domain adaptation [10].

In particular, methods for the weakly supervised detection of objects have been developed to deal with domain adaptation. But while this problem has been extensively studied for photographic images, much less attention has been paid to WSOD in the case of strong domain shifts, as in the case of non-photographic images, possibly including domain-specific visual category. Some works focus on cross-domain weakly supervised object detection (i.e. where bounding boxes are available for the same visual category but in an other domain than the target one), as in [11, 12].

In this work, we take interest in weakly supervised object detection in the case of extreme domain shifts, namely non-photographic images, possibly addressing the detection of new, never seen classes. We claim that an efficient way to perform this task is to rely on a simple Multiple Instance Learning (MIL) paradigm that is applied directly to the deep features of a pre-trained network. This approach does not involve any cross-domain learning step and can therefore be applied to arbitrary datasets and classes. Beside being efficient, as we will see in the experimental section, such a strategy also enables one to have relatively small training times. First, no fine-tuning is involved and second, we introduce a MIL strategy that is much lighter than the classical SVM approaches [13].

In order to illustrate the usefulness and efficiency of the approach, we focus on databases of man-made images, namely paintings, drawings, cliparts or comics. This poses a serious challenge because of both the lack or scarcity¹ of annotated databases and the great variety of depicting styles. Being able to detect objects in such image modality has become an important issue, mostly because of the large digitization campaigns of fine arts. These include digital scans and photographs of artworks (mainly done by the museums and other public institutions) and scans of archive photographs (such as the Cini Foun-

¹Classical databases used for training networks are made of millions of natural images (Imagenet [14](millions of images), PASCAL VOC [15], MS COCO [16] Google Open Image Dataset (9M images) [17]). In contrast, datasets for recognition in non-photographic images are rare and usually only containing image-level annotations, as in the iMet dataset (375k) [18] or BAM! (2.5M) [19]. The very few datasets with bounding boxes such as PeopleArt [20], used later in this paper, are very small.

ation archive [21]). Such digital collections allow the preservation and remote access to cultural heritage, as embodied for instance by the IIF community².

In a previous conference paper [22] we have shown that the proposed method is a valid strategy when dealing with extreme domain shifts. In this paper, we fully develop the approach, exploring several extensions of the model such as a multi-layers version of the Multiple Instance perceptron and a polyhedral version obtained by aggregating several linear classifiers. We also thoroughly evaluate the performances of the approach by comparing it to several state-of-the-art approaches on databases with challenging domain shifts, including paintings, drawings and cliparts. The experimental section shows that in such cases, the approach outperforms methods specially developed for the considered databases, as well as classical MIL approaches and some state-of-the-art WSOD approaches.

The paper is organized as follows. In the next section we review WSOD algorithms and MIL methods as well as some deep learning applications to recognition tasks in non-photorealistic images. In section 3, we then present our algorithm as well as some of its variants. In section 4, extensive experiments are presented, including comparisons to alternative algorithms and study of sensitivity of our method to its parameters.

2. Related Work

In this section we first review some state-of-the-art WSOD algorithms (an exhaustive review of this field is beyond the scope of the paper) and then explore MIL methods. Eventually, we make a brief survey of applications of deep learning for visual recognition in non-photographic images.

2.1. Weakly Supervised Object Detection

Computer vision methods often treat WSOD as a Multiple Instance Learning (MIL) problem [23], especially in realistic cases where objects are not necessarily centered and with cluttered background [24, 25, 26, 4]. In such cases, the image is viewed as a collection of potential instances of the object to be found (for example crops of various sizes and positions). A sketch of a typical weakly supervised detector is as follows :

1. Proposal generation : extract a certain number of regions of interest from the image.
2. Feature extraction : compute a feature vector per region (off the shelf, handcrafted, CNN based...).
3. Classification : this is often done with a MIL algorithm to obtain an instance classifier.

²<https://iif.io/>

These general steps can be alternated or entangled (for example to enhance the region proposition or feature extraction parts based on the performance of the final classifier). In [26] steps 1 and 2 are handled by extracting the features (and regions) proposed by RCNN [27]. These features are passed to a smoothed version of SVM that serves as a MIL algorithm. Particular attention is paid to the initialization phase, which is crucial due to the fact that the MIL problem is essentially non-convex even if the SVM algorithm is.

More recent methods tend to entangle all the mentioned steps in an end-to-end manner. For instance, some CNN based methods group feature extraction and classification [4, 28, 29, 30] whereas others group the three steps together [5]. In [4] Bilen and Vedaldi propose a Weakly Supervised Deep Detection Network (WSDDN) based on Fast RCNN [31]. It consists in transforming a pre-trained network by replacing its classification part by a two streams network (a region ranking stream and a classification one) combined with a weighted MIL pooling strategy. This work has been improved in many ways [32, 29, 33, 34, 35, 36]. For instance, Tang et al. [37] refine the prediction iteratively through multistage instance classifier. Later, this model was improved by adding a clustering of the region proposals [6]. In [32], the WSDDN model has been improved by adding two entropy term at the loss function to minimize the randomness of object localization during learning, whereas in [36], the authors propose to tackle the non-convexity of the MIL pooling by using a series of smoothed loss functions.

In [38], a two steps strategy is proposed, first collecting good regions by a mask-out classification, then selecting the best positive region in each image by a MIL formulation and then fine-tuning a detector with those propositions acting as ground truth bounding boxes. This pseudo-labeling step is often used in the weakly supervised pipeline. In [5] a region proposal generator is built using weak supervision. The feature maps are transformed into a graph then into an objectness score map. This objectness score ponderates the feature maps that are subsequently fed to a classification layer. In [39] the authors proposed to train two collaborative networks one of it being a Conditional Network with noisy extra-channel. The goal is to jointly minimize the dissimilarity between the prediction distribution and the conditional distribution.

It is worth noting that although CNN feature maps contain some localization information [40], the main difficulty for weakly supervised detection is the construction of an efficient box proposal model. Most works in the field use effective unsupervised methods for region proposals such as Selective Search [41] or EdgeBoxes [42].

2.2. *Generic Multiple-Instance Learning*

As stated above, the problem of weakly supervised object detection can be recast into a multiple instance learning (MIL) problem [23]. More precisely, we are interested in instance classification as opposed to bag classification. We want to find an object among several candidate boxes in order to detect the object of interest. In [13] a solution based on iterative applications of a Support Vector Machine (SVM) has been proposed to solve the MIL problem. Actually two flavors are considered, mi-SVM and MI-SVM. In the case of mi-SVM, each

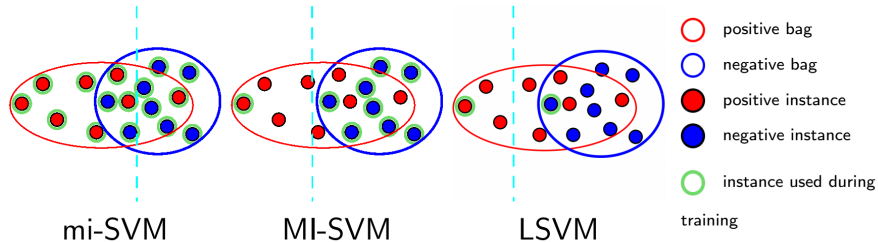


Figure 1: Comparison of standard SVM based MIL models. The blue dotted lines show the hyperplanes learned by the models, and the blue circles show the instances used during the SVM training. Figure must be seen in color.

element of positive bags is assigned a label and the SVM margin is imposed at the instance level. In the case of MI-SVM, the SVM margin is imposed the most positive element of each positive bag and to the least negative element of each negative bag. In both cases, at test time, the learned classifier can be applied at the instance level. In [43] a reformulation of MI-SVM is proposed and called latent SVM (LSVM). But in this work, a bag of instance represents the set of parts of an object and the MIL formulation is used to train an object detector with a fully-supervised training.

Several heuristics to solve the non convex-problem posed by the MIL have been proposed. For example, in [44] is introduced a new objective function that try to estimate the quantity of positive examples in a positive bag, before using deterministic annealing to optimize it. In contrast to the MI-SVM method, the algorithm can consider several elements as positive in the positive bag. In [45], the authors propose a convex relaxation of the softmax loss. A comprehensive review of SVM based MIL methods can be found in [46]. From this review it appears that mi-SVM and MI-SVM are still competitive on the tasks studied there.

Figure 1 summarizes the instances on which the SVM margins are imposed in the most popular SVM based MIL methods.

Another approach to the MIL problem is to use neural networks whose architecture treats each instance symmetrically, before an explicit aggregation (max, average) is performed. From this point a classical neural network performs a classification task [47, 48]. An improvement using more recent deep learning building blocks is proposed in [49]. The aforementioned works did not focus on the instance classification performance. They all, by design, provide an instance classification network (present the network with a bag consisting of one item).

From a recent survey [50] on multiple Instance Learning it appears that the most efficient algorithm for an instance level classification seems to be a clever variation of bagging and multiple classifiers to deal with multi-modal distributions [51].

Based on these surveys, we are driven to propose a method that mimics an SVM within a neural network. The main difference between our approach

and the SVM based MIL methods is that iterations are performed during the training of the neural network and the multi-modal nature of the objects to be found drives us to consider multiple linear classifiers of each considered class.

2.3. Deep Learning for visual recognition in non-photographic images

As almost all applications of computer vision, tasks dealing with hand-drawn or computer generated non-photographic images benefited from the resurgence of neural networks. One point in common between all works in the field is the reuse of architectures that were originally designed for photographs classification. Some works use the pre-final features of a network as the only features retained to represent an image and do not fine-tune the network for the task at hand. Other methods allow for a certain amount of fine-tuning and add a specific network after the original architecture. Another significant difference between the papers we are going to cite is whether or not the considered classes were present in the training dataset of the original network. In the simplest setting, features from a pre-trained network are retained and used to train a linear SVM [52, 53], the task being the recognition of classes already present in the original training set the network was pre-trained on.

Several works have also shown that pre-trained CNN architecture can be efficiently transferred for learning new semantic visual categories, those networks either being used as features extractors [52, 53] or being fine-tuned [54, 55, 19].

A large body of works investigate the fine-tuning of CNN for style recognition [56, 57, 58], material [59], scene [60] or author classification [61]. The use of CNN also opens the way to efficient artwork analysis tasks, such as visual links retrieval [62], posture estimation [63], visual question answering [64] and instance recognition [65, 66]. Some works try to tackle several of those tasks at the same time [67, 68]. A survey about machine learning for cultural heritage have been recently published [69].

The object detection problem (recognize and locate an object) in artworks has been less studied. In [20] and [55] it is proposed to fine-tune a detection network in a fully supervised manner to detect people and classical Pascal VOC classes, respectively. In [11], an efficient pipeline is proposed to train a detector on new artistic modalities in a semi-supervised manner. This approach requires natural images with bounding boxes annotation of those classes and involves a relatively costly style transfer procedure. In particular, this method only allows the detection of object classes that are present and have been annotated in natural images. This specific problem has been recently studied by different research teams [70, 12]. The same is true for many works focusing on recognizing the same object categories in different modalities [71, 19, 72]. Only very few works have focused on visual categories that are new and specific to artworks [73, 22]. In [73], the authors proposed an interactive search engine to detect objects in artistic images for object categories such as praying hands, cross or grape. In [22], the authors proposed a simple MIL classifier coupled with Faster RCNN [1] to weakly learn to detect new visual categories such as Mary or Saint Sebastian. The present work extends the MIL model proposed in this paper

by allowing polyhedral classification and evaluate its performances on various modality such as paintings, drawings or cliparts.

3. Multiple instance perceptron for the weakly supervised detection of objects

In this section, we present the main multiple instance model that we propose, together with several of its variants. For the task of instance level classification, this model can be used to weakly transfer an object detector to a new domain or to new visual categories. We begin by introducing the notations, then our model and the intuitions behind it. Finally, we compare our model with existing Multiple Instance networks.

3.1. The MIL framework

We first give some basic notations related to Multiple Instance Learning. Let $\mathcal{B} = \{B_1, B_2, \dots, B_N\}$ a set composed of N bags. Each bag B_i corresponds to a positive or negative label $Y_i = \{-1, 1\}$ and contains K_i feature vectors : $\{X_{i,1}, X_{i,2}, \dots, X_{i,K_i}\}$ where $X_{i,k} \in \mathbb{R}^d$. Each of these feature vectors (instances) corresponds to a positive or negative label. Instance labels are unknown in positive bags, but are assumed negative in negative bags. A common hypothesis (called MIL assumption) is that a bag is labeled positive if at least one instance contained in the bag is labeled positive :

$$Y_i = \begin{cases} +1 & \text{if } \exists k \in \{1, \dots, K_i\} : y_{i,k} = +1 \\ -1 & \text{if } \forall k \in \{1, \dots, K_i\} : y_{i,k} = -1 \end{cases}$$

where $y_{i,k}$ denotes the instance label. In an object detection setting each feature vector will represent a region. As in a typical classification problem, the goal is to learn a prediction function f_w , parametrized by w , so that the predicted output $f_w(X) = \hat{y}$ minimizes the empirical risk. The typical way to do so is to minimize a loss function that measures the correctness of the prediction over the training examples.

However, in the Multiple Instances setup, we only have bag-level information during training, whereas we are looking for an efficient instance level prediction. Observe also that in this work, we are interested in the instance level classification task (in order to be able to classify each vector and hence each region of the image) and not in the bag-level one, which is also classical in MIL applications. There are two main ways to tackle the fact that we only have bag level ground truth information.

First, one can aggregate all the predictions of one bag to a single prediction (at bag level) during training. Hence we can write $\hat{y}_i = g(\{\hat{y}_{i,k}\}_{k \in \{1 \dots K_i\}})$ with g an aggregation function over the elements of a bag i . In this case, the loss function can be written as $L(Y_i, \hat{y}_i) = l(Y_i, g(\{\hat{y}_{i,k}\}_{k \in \{1 \dots K_i\}}))$. The best way to aggregate instance level predictions in order to find a classifier separating each of the individual vectors $X_{i,k}$ of each bag at test time is still an open-problem. Works use the max operator [48], the average or the Log-Sum-Exponential [47]

for g . Indeed, since the training is done with only bag level information, at test time the learned classifier must be able to handle each instance almost independently from the others because of the variety of objects that may appear in test image.

Second, one can consider each instance of a bag individually (as in the mi-SVM case, see Figure 1) and the loss function can be written as $L(Y_i, \{y_{i,k}\}_{k \in \{1 \dots K_i\}}) = g(l(h_{i,k}(y_i), \{y_{i,k}\}_{k \in \{1 \dots K_i\}}))$ where g is an aggregation function (usually an average), l a penalty function and $h_{i,k}$ a modification function of the label associated to the instance, usually named a latent label [43]. If we consider that the label of a bag is equal to the label of its instances, $h_{i,k}$ is the identity, otherwise it is a function from $\{-1, 1\}$ to $\{-1, 1\}$ depending on the bag and the instance.

3.2. Multiple Instance solution for the WSOD task

3.2.1. The main model : a multiple instance perceptron

Instead of the classical SVM generalization for MIL proposed in [13] and based on costly iterations of SVM, we propose a simple model which is a multiple instance extension of the perceptron [74] with a maximum taken over the instances of a bag. Our model can be seen as a latent perceptron if we use the same designation as [43]. It is also similar in spirit to the MI-network proposed by [48]. We denote our model **MI-max**³ as introduced in [22]. As we consider each class individually, we focus on the case of binary classification.

We build on a linear model $f_w(X_{i,k}) = W^T X_{i,k} + b$ with $W \in \mathbf{R}^M$, $b \in \mathbf{R}$, which we combine with a maximum aggregation function $g = \max_{k \in \{1 \dots K_i\}}$ and a per example loss function equal to

$$l(y, \hat{y}) = 1 - y \text{Tanh}(\hat{y}) = 1 - \text{Tanh}(y\hat{y}). \quad (1)$$

We also use a regularization term on the norm of W and a weighting of the two classes, so that the complete loss function is :

$$\mathcal{L}(W, b) = 2 - \sum_{i=1}^N \frac{y_i}{n_{y_i}} \text{Tanh} \left(\max_{k \in \{1 \dots K_i\}} (W^T X_{i,k} + b) \right) + C \|W\|^2, \quad (2)$$

with n_1 the number of positive examples in the training set and n_{-1} the number of negative examples.

As mentioned before, the intuition behind this formulation is that minimizing $\mathcal{L}(W, b)$ amounts to seek a hyperplane separating the most positive element of each positive image from the least negative element of the negative image (i.e. from all examples in the negative bags). Also this loss seeks to maximize the margin.

The regularization term apart, this loss function equals 0 if and only if the classification is perfect. In the worst case scenario, its value is 4 (plus the

³When it is not mentioned, the model uses the objectness score such as in section 3.2.2.

regularization term). Furthermore, if the hyperplane $W^T X + b = 0$ exactly separates the most positive examples of each positive bag from the set of all examples of all negative bags, then replacing C, W and b by $\lambda C, \frac{1}{\lambda} W$ and $\frac{1}{\lambda} b$ respectively and taking λ to 0 will lead to a loss as close to 0 as desired. This implies that if the MIL problem admits an exact linear solution, then our loss accepts it provided C is small enough.

One advantage of this formulation is that it can be tackled by a simple gradient descent, therefore avoiding the very costly iterative procedures of other MIL solutions such as [13]. Taking the max over all instance of a bag is akin to what is done in MI-SVM (mentioned in section 2.2) when after each full training of an SVM, a new representative element of each bag is selected for the next SVM training. We can switch to a stochastic gradient descent by iterating on random batches when the dataset is too big. Of course, since our loss is not convex, we are not guaranteed to find the global minimizers of the function. To tackle this problem, we run r times the model with a random initialization and pick the best one on the training set evaluation of the loss function.

If we refer to the simple description of the WSOD standard pipeline, we only focus on the multiple instance classification task and not on the boxes proposals algorithms, features extraction or refinement methods mentioned section 2.1.

3.2.2. From MIL to WSOD

In the context of Weakly Supervised Object Detection (WSOD), each bag i corresponds to an image and each instance k corresponds to a candidate region to be labeled. We here assume that candidate regions are returned by a classical detection network, together with features and a class-agnostic objectness score, but without any label. That is, we ignore the classification ability of the detection network. Training a WSOD model from scratch, especially when the database is rather small and from another domain, is a very hard problem. Thus, reusing as much as possible models that have been trained on large datasets is advisable.

The idea is to give more importance to the classification of boxes with the highest objectness score. We observed that using the class-agnostic objectness score attached to each proposed box consistently gave better results (see section 4.3.1). We chose to multiply each $W^T X_{i,k} + b$ by the objectness score of the region k before taking the maximum :

$$f_w(X_{i,k}) = (s_{i,k} + \epsilon) (W^T X_{i,k} + b), \quad (3)$$

with $\epsilon \geq 0$ and where $s_{i,k}$ is a class-agnostic objectness score of the region k , as returned by the detection network. The motivation behind this formulation is that the score $s_{i,k}$, roughly a clue that there is an object in box k , provides a prioritization between boxes. The same idea is used in the WSDDN model [4] or in MELM [32].

At test time, the instance level decision is made as before according to the sign of $(W^{*T} x + b^*)$, since multiplication by a positive score does not change the sign. Indeed, the hyperplane W^*, b^* is chosen to separate two classes and the

loss \mathcal{L} aims at maximizing the margin with respect to this hyperplane. It stands to reason that the instance level classification must be related to the relative position of the instance and the hyperplane. Nevertheless, we will propose in section 4 a non maximal suppression strategy that will once again use the objectness score to filter the boxes proposed for each class. More precisely the non maximal suppression algorithm will use the following score :

$$S(x) = \text{Tanh}\{(s(x) + \epsilon) (W^{*T} x + b^*)\} \quad (4)$$

which mixes the objectness score $s(x)$ and the signed distance from the hyperplane $W^{*T} x + b^*$.

We now present two natural extensions of our core model. We first make use a neural network to transform the bare features $X_{i,k}$, so that the transformed features can be more relevant to the task at hand. Then, we investigate the interest of a polyhedral separation instead of a hyperplane for classification.

3.2.3. One hidden layer network

In this extension, called **MI-max-HL**, the bare features $X_{i,k}$ are transformed by a hidden layer before the MI-max approach is applied. This can be summarized by modifying the function f_w as follows :

$$f_w(X_{i,k}) = \Omega^T (\text{Tanh}(W^T X_{i,k} + b)) + \beta,$$

with $W \in \mathbf{R}^{L \times M}$, $b \in \mathbf{R}^L$, $\Omega \in \mathbf{R}^L$, $\beta \in \mathbf{R}$ and L the dimension of the hidden layer. When compared with MI-max the parameters to be learned are Ω, β, W, b for a total dimension of $L + 1 + L \times M + L = L \times (M + 2) + 1$ compared to the original $M + 1$ scalars.

3.2.4. Multiple linear classifier Model

As mentioned in the introduction, an improvement of the linear model consists in learning several hyperplanes in parallel, so that the binary classification is performed in a collaborative manner instead of selecting the best hyperplane. The contributions of several hyperplanes are gathered with a maximum function, so that the model can be defined as :

$$f_w(X_{i,k}) = \max_{j \in \{1 \dots r\}} (W_j^T X_{i,k} + b_j)$$

At each iteration of the gradient descent only one of the couple (W_j, b_j) is updated. For the inference the r hyperplanes are used.

This model, named **Polyhedral MI-max** yields a concave polyhedral boundary between the two classes. The concept of convex polyhedral separability has been introduced by [75] and well studied in the framework of polyhedral and piece-wise linear classifier. In our case, this allows one to get more complex boundary at a modest extra-cost compared to a kernel SVM.

Those different models will be experimentally compared in section 4.

4. Experiments

4.1. Experimental Setup

Features extraction : We use the Faster RCNN detection network [1] as a feature extractor and region proposal algorithm. We extract 300 regions per image along with their high-level features⁴ and the class-agnostic objectness score attached to each proposed box by the Region Proposal Network (RPN). Let us stress that, by using Faster R-CNN, our system uses a subpart that has been trained on databases with bounding boxes ground truth. In WSOD setups such as [4, 5, 76], the models have not seen any bounding boxes, even on different modality. Observe nevertheless that, in contrast with domain adaptation methods such as [11], our method allows the detection of new classes.

According to [77], the ResNet family of networks appears to be the best architecture for transfer learning by feature extraction. Among this family we chose ResNet 152 layers trained on MS COCO [16]. Therefore, the backbone we used has been trained on ImageNet, then fine-tuned on MS COCO. Remember that we chose not to fine-tune the backbone in order to provide a fast and flexible tool that can be used on small data sets. As a consequence, the backbone of our model only saw photographs for its two-phase training (ImageNet, MS COCO).

Parameters of the models : For training our MIL models, we use a batch size of 1000 examples (for smaller sets, all features are loaded into the GPU), 300 iterations of gradient descent for the linear model, performed with a constant learning rate of 0.01 and $\epsilon = 0.01$ and $C = 1$ (equations (3) and (2)). The complete training takes about 6 minutes for 7 classes on the IconArt dataset [22] with 12 random starting points per class using a consumer GPU (GTX 1080Ti). In the case of Polyhedral MI-max and MI-max-HL we used 3000 iterations which increase the training time to 1 hour. For MI-max-HL, we use a maximum batch size of 500 elements. Actually, the random restarts and classes are performed in parallel to take advantage of the presence of the features in the GPU memory, thus reducing the GPU-CPU transfer times. Typically, 20 classes can be learned in parallel on a standard GPU, due to the light weight of the model. One of other the advantage of not fine-tuning the network is that there is no need to store the heavy weights of the new trained model.

Comparison to multiple instance neural networks :

The MIL part of our model MI-max-HL is close in spirit to the multiple instance neural networks proposed by [47] and [48] and further extended in [49]. None of these authors use the approach for weakly supervised object detection. Nevertheless, we will include in the experimental comparisons some applications (that we will call `MI_net` or `mi_net`) of this MIL methodology to the same deep features as in our method. This can be seen as an extension of the general approach proposed in this paper.

⁴The output of layer `fc7` often called 2048-D.

4.2. Results and comparison to other methods

In this section, we perform weakly supervised object detection experiments on different databases. We compare our different models MI-max, Polyhedral MI-max and MI-max-HL, to the three types of methods.

The first group of methods are those specifically targeted at WSOD using fine-tuned networks. We have included state-of-the-art methods for which a source code is available: Soft Proposal Network (SPN [5]) and Proposal Cluster Learning (PCL [76]). For some of the datasets, we also include results from the Weakly supervised detection network (WSDDN [4]) from [11]. For those datasets we also show the performance obtained by the mixed supervised method with domain adaptation proposed by [11], a method that assume that datasets with bounding boxes for the same classes on different modality are available.

The second family of methods are generic MIL-methods directly applied to the set of deep features vectors generated by Faster RCNN. Observe that these methods ignore the objectness scores returned by the detection network. The first ones are MI-SVM and mi-SVM from [13]. These two methods require to train several SVMs and are therefore costly. In some cases (for the datasets PeopleArt and IconArt) we performed a PCA on the training set to reduce the number of components from 2048 to around 650 dimensions by keeping 90% of the variance (to fit on SVM in CPU memory). We experimentally observed on the other datasets that this dimensionality reduction doesn't reduce the performances. Eventually, the computationally lighter MI_Net, MI_Net with Deep Supervision (DS) or Residual Connection (RC) and mi_Net from [49] are also considered. Although those models are designed for bag level classification, we used them for instance level prediction. Again, these can be seen as variants on the method we develop in this paper (the weakly detection of objects is not addressed in [49]).

The last type of methods are those who (before any training) use the objectness score of the proposed regions to keep only one feature vector for each positive image. The method MAX keeps one feature vector per image and learns a linear SVM classifier that separates the positive vectors from the negative one [78]. The variant MAXA also keeps one vector per positive image but uses all vectors from the negative ones. Again, a linear SVM is learned. In both cases a 3-fold cross validation is performed.

At test time, the labels and the bounding boxes are used to evaluate the performance of the methods in term of Average Precision par class. The generated boxes are filtered by a NMS with an IoU threshold of 0.3 [15] and a confidence threshold of 0.05 for all methods.

Table 1: Overall information of the evaluated datasets.

Reference	Dataset	# Images in train	# Images in test	# Instances in test	# Classes	Min # Images per class	Classes from natural images	Classes from Pascal VOC
[20]	PeopleArt	3007	1616	1137	1	968	Yes	Yes
[11]	Watercolor2k	1000	1000	3315	6	27	Yes	Yes
[11]	Clipart1k	500	500	3615	20	21	Yes	Yes
[11]	Comic2k	1000	1000	6389	6	87	Yes	Yes
[72]	CASPA paintings	1045	1033	1486	36	8	Yes	6 out of 8
[22]	IconArt	2978	1480	3009	7	75	No	No

Table 2: **People-Art (test set)** Average precision (%). Comparison of the proposed MI-max, Polyhedral MI-max and mi-perceptron methods to alternative approaches. In red the best weakly supervised method.

Network	Method	Model	person
VGG16-IM	Weakly supervised fine tuning	SPN [5]	10.0
		PCL [76]	3.4
RES-152-COCO	Features extraction	MAX [78]	25.9
		MAXA	48.9
		MI-SVM [13]	13.3
		mi-SVM [13]	5.6
		MLNet [49]	33.0 ± 6.0
		MLNet_with_DS [49]	19.5 ± 11.4
		MLNet_with_RC [49]	12.5 ± 8.3
		mi_Net [49]	26.5 ± 8.5
		MI-max	55.5 ± 1.0
		Polyhedral MI-max	58.3 ± 1.2
MI-max-HL	57.3 ± 2.0		

Table 3: **Watercolor2k (test set)** Average precision (%). Comparison of the proposed MI-max, Polyhedral MI-max and mi-perceptron methods to alternative approaches. In green the best mixed supervised method and in red the best weakly supervised one.

Net	Method	Model	bike	bird	car	cat	dog	person	mean
SSD	Mixed supervised with domain adaptation	DT+PL [11] ⁵	76.5	54.9	46.0	37.4	38.5	72.3	54.3*
VGG16-IM	Weakly supervised fine tuning	WSDNN [4] ⁵	1.5	26.0	14.6	0.4	0.5	33.3	12.7
		SPN [5]	0.0	18.9	0.0	0.0	0.0	23.6	7.1
		PCL [76]	0.0	0.0	0.0	0.0	0.0	0.0	0.0
RES-152-COCO	Features extraction	MAX[78]	76.0	33.8	33.0	20.8	22.7	19.8	34.3
		MAXA	60.6	39.2	39.6	30.9	32.0	61.2	43.9
		MI-SVM [13]	66.8	20.9	7.6	14.1	8.5	13.2	21.8
		mi-SVM no GS [13]	10.6	10.9	1.4	2.0	0.8	5.9	5.3
		MLNet [49]	77.6	32.4	35.5	24.7	16.2	18.0	34.1 ± 1.0
		MLNet_with_DS [49]	73.4	22.4	25.8	17.6	11.2	10.3	26.8 ± 2.4
		MLNet_with_RC [49]	32.3	19.2	20.1	6.7	6.8	15.4	16.7 ± 6.3
		mi_Net [49]	66.4	30.3	14.9	14.4	8.6	20.5	25.8 ± 3.5
		MI-max	84.1	47.4	48.2	30.9	27.9	58.2	49.5 ± 0.9
		Polyhedral MI-max	77.8	44.7	45.5	25.6	26.7	59.2	46.6 ± 1.3
MI-max-HL	79.3	46.1	43.6	26.9	28.8	57.0	47.0 ± 1.6		

Table 4: **Clipart1k (test set)** Average precision (%). Comparison of the proposed MI-max, Polyhedral MI-max and mi-perceptron methods to alternative approaches. In those case, we use a grid search for MAX and MAXA. In green the best mixed supervised method and in red the best weakly supervised one.

Net	Method	Model	airplane	bicycle	bird	boat	bottle	bus	car	cat	chair	cow	diningtable	dog	horse	motorbike	person	potteryplant	sheep	sofa	train	tvmonitor	mean
SSD	Mixed supervised with domain adaptation	DT+PL [11] ⁵	35.7	61.9	26.2	45.9	29.9	74.0	48.7	2.8	51.0	72.7	50.2	19.3	40.9	83.3	62.4	42.4	22.8	38.5	49.3	56.5	46.0*
YOLOv2		DT+PL [11]																					30.9*
FastRCNN		DT+PL [11] ⁶																					34.9*
VGG16-IM	Weakly supervised fine tuning	WSDNN [4] ⁵	1.6	3.8	0.6	2.3	0.1	11.7	4.5	0.0	4.2	0.1	2.8	2.3	0.0	0.1	14.4	16.0	4.5	0.7	1.2	16.3	4.4
		SPN [5]	0.0	12.5	0.8	0.1	0.0	12.5	1.0	0.0	0.1	4.8	6.4	0.0	5.3	0.0	0.0	0.0	0.0	0.0	21.5	2.5	3.8
		PCL [76]	0.4	0.0	0.3	1.1	0.1	0.0	5.9	0.0	0.0	0.0	0.0	0.2	3.8	0.3	0.0	3.6	1.5	0.0	0.7	0.0	1.4
RES-152-COCO	Features extraction	MAX[78]	15.2	12.6	15.2	23.1	2.2	34.5	10.0	0.0	15.6	7.7	2.4	4.6	21.2	01.9	15.4	32.6	0.4	0.0	60.4	22.9	16.9
		MAXA	24.7	29.7	19.7	31.6	6.0	37.0	14.6	0.0	30.6	1.7	4.2	0.0	12.7	03.0	35.4	34.0	0.7	4.9	50.3	29.5	22.0
		MI-SVM [13]	10.8	30.8	3.4	22.1	15.6	29.8	8.9	26.9	4.8	14.3	0.0	18.4	16.0	22.6	16.4	1.8	7.9	31.9	22.4	18.3	18.3
		mi-SVM no GS [13]	1.0	4.1	8.1	6.4	1.5	4.5	16.0	4.4	10.4	4.1	2.7	0.1	10.6	20.5	6.2	3.1	0.2	2.6	8.6	8.5	6.2
		MLNet [49]	21.3	45.6	26.8	22.2	37.4	47.6	28.8	18.4	40.0	20.1	21.7	4.3	24.6	24.3	27.9	22.2	7.2	29.7	67.0	53.9	29.7 ± 1.5
		MLNet_with_DS [49]	12.9	44.1	15.0	12.1	25.1	30.5	11.8	14.0	26.4	14.4	16.8	4.3	8.9	12.6	16.4	15.2	5.1	23.5	30.5	39.1	18.9 ± 2.4
		MLNet_with_RC [49]	1.6	2.0	0.2	0.0	0.6	0.1	3.2	0.4	0.6	0.6	0.1	0.0	0.5	0.3	2.2	1.9	0.3	0.6	2.3	0.0	0.9 ± 0.8
		mi_Net [49]	20.0	43.6	28.7	23.0	30.3	36.4	13.2	20.2	42.6	14.3	25.7	3.9	22.1	21.2	30.3	9.7	5.8	28.0	41.3	25.2	29.5 ± 1.2
		MI-max	42.4	46.4	25.0	45.6	45.6	52.6	33.7	34.0	45.5	42.4	29.1	5.9	35.5	52.3	55.5	50.0	2.1	15.7	60.3	47.9	38.4 ± 0.8
		Polyhedral MI-max	20.6	39.6	3.6	34.3	41.4	50.7	30.8	1.7	30.9	35.1	1.6	0.0	24.6	26.6	55.4	26.2	4.0	7.6	50.1	42.0	30.6 ± 0.0
MI-max-HL	31.8	46.6	25.5	31.3	45.1	41.6	43.1	8.6	46.9	33.9	8.7	3.7	29.8	43.5	54.4	51.9	2.7	14.6	48.6	47.7	33.0 ± 1.2		

As explained above, we concentrate on non-photographic databases for which a ground truth is available for object detection on the test set. We report in Tables tables 2 to 7 the performances for the weakly supervised object detection

⁵The performance comes from the original paper [11].

⁶The performance comes from the original paper [11].

⁷The performance comes from the original paper [11].

⁸Trained with the following hyperparameters : batch size = 2, learning rate = 0.001, epochs = 13 and number of clusters by default.

Table 5: **Comic2k (test set)** Average precision (%). Comparison of the proposed MI-max method to alternative approaches. no GS means no Grid Search on the hyperparameters of the SVM otherwise it is the case.

Net	Method	Model	bike	bird	car	cat	dog	person	mean
SSD	Mixed supervised with domain adaptation	DT+PL [11] ^r	76.5	54.9	46.0	37.4	38.5	72.3	54.3*
VGG16-IM	Weakly supervised fine tuning	WSDDN [4] ^r	1.5	26.0	14.6	0.4	0.5	33.3	12.7
		SPN [5]	0.0	0.0	0.0	3.1	0.0	4.1	1.2
		PCL [76]	0.0	0.0	0.0	0.0	0.0	0.0	0.0
RES-152-COCO	Features extraction	MAX[78]	15.2	2.7	29.4	2.3	16.8	4.9	11.9
		MAXA	36.8	5.6	27.1	8.2	6.1	34.8	19.8
		MI-SVM [13]	34.2	3.0	20.0	5.2	2.5	12.9	13.0
		mi-SVM no GS [13]	10.8	2.3	5.5	3.2	2.1	3.6	4.6
		MLNet [49]	42.9	15.5	33.1	11.8	13.4	20.4	22.8 ± 1.1
		MLNet_with_DS [49]	40.8	13.3	32.5	5.7	9.1	16.1	19.6 ± 1.6
		MLNet_with_RC [49]	19.8	5.4	16.4	2.8	9.8	13.9	11.4 ± 4.4
		mi_Net [49]	42.1	10.9	24.5	8.8	8.8	22.1	19.5 ± 2.1
		MI-max	45.3	9.7	33.7	14.4	21.6	37.0	27.0 ± 0.8
		Polyhedral MI-max	39.2	2.8	32.5	11.6	18.9	39.5	24.1 ± 0.0
		MI-max-HL	43.0	5.1	31.5	11.8	13.8	36.4	23.6 ± 0.5

Table 6: **CASPA paintings (test set)** Average precision (%). Comparison of the proposed MI-max method to alternative approaches. no GS means no Grid Search on the hyperparameters of the SVM otherwise it is the case.

Net	Method	Model	bear	bird	cat	cow	dog	elephant	horse	sheep	mean
VGG16-IM	Weakly supervised fine tuning	SPN [5]	0.5	0.1	1.6	0.9	0.5	1.4	0.6	0.0	0.7
		PCL [76]	0.0	0.0	0.0	0.0	0.0	0.0	0.0	0.0	0.0
RES-152-COCO	Features extraction	MAX[78]	22.0	2.1	14.5	3.5	14.2	8.8	12.8	0.5	9.8
		MAXA	26.3	13.1	26.9	5.4	8.3	18.1	14.9	3.9	14.6
		MI-SVM [13]	9.3	0.2	6.7	1.5	0.1	0.6	0.9	0.4	2.5
		mi-SVM no GS [13]	1.3	1.6	3.0	0.8	1.0	0.3	1.5	0.3	1.2
		MLNet [49]	32.8	5.4	14.1	5.2	6.2	15.0	11.1	4.2	11.7 ± 1.6
		MLNet_with_DS [49]	29.0	1.6	8.3	3.0	3.2	5.9	7.1	2.6	7.6 ± 1.2
		MLNet_with_RC [49]	16.9	0.9	6.6	2.6	2.9	8.2	4.7	2.1	5.6 ± 2.1
		mi_Net [49]	26.7	8.9	12.5	1.5	3.4	7.1	5.1	2.4	8.4 ± 1.7
		MI-max	28.3	15.7	25.6	5.3	13.7	17.2	18.8	5.1	16.2 ± 0.4
		Polyhedral MI-max	25.6	17.2	23.0	4.4	14.8	7.5	17.4	5.0	14.4 ± 0.0
		MI-max-HL	26.5	15.7	26.3	4.8	14.2	10.1	11.5	6.2	14.4 ± 0.9

task for 6 different non-photographic datasets : PeopleArt [20], Watercolor2k, Clipart1k, Comic2k [11], IconArt [22] and CASPApaintings [72]. CASPApaintings is the paintings subset of the CASPA dataset⁹ proposed in [72] with bounding boxes associated to 8 visual categories (only animals) for most of the images.

When the method is not too costly we provide standard deviation and mean score computed on 10 runs of it.

First, we can see that for all databases, the end-to-end weakly supervised methods (WSDDN, SPN and PCL) yield relatively poor results. Possible explanations are that the model overfits on the training set or that the model is stuck in bad local minima, so that the weakly supervised setting is not adequate with a relatively small training dataset. Moreover in the case of PCL, the boxes are proposed by the Selective Search algorithm [41] which, as shown in Table 11, completely fails on the considered non-photographic datasets. That alone can explain the poor results of PCL on those datasets. Recall also that these methods do use features inherited from systems such as FasterCNN that are pretrained with bounding box annotations.

When comparing the performances of the different multiple instance neural networks, we can see that MLNet (Maximum Bag Margin Formulation) out-

⁹http://people.cs.pitt.edu/~chris/artistic_objects/

Table 7: **IconArt detection test set** *detection* average precision (%) at IoU ≥ 0.5 . Comparison of the proposed MI-max, Polyhedral MI-max and mi-perceptron methods to alternative approaches. In those case, we use a grid search for MAX and MAXA. In red, the best weakly supervised method.

Net	Method	Model	angel	JCchild	crucifixion	Mary	nudity	ruins	StSeb	mean
VGG16-IM	Weakly supervised fine tuning	SPN [5]	0.0	0.8	22.3	12.0	6.8	10.4	1.2	7.7
		PCL ⁸ [76]	2.9	0.3	1.0	26.3	2.3	7.2	1.4	5.9
RES-152-COCO	Features extraction	MAX[78]	1.4	1.3	11.5	2.8	3.8	0.3	4.5	3.7
		MAXA	1.3	4.4	18.2	28.0	15.3	0.2	16.4	12.0
		MI-SVM [13]	0.7	4.4	21.6	0.6	1.0	0.0	0.0	4.0
		mi-SVM [13]	1.3	5.1	3.9	3.6	2.9	0.3	2.2	2.8
		MLNet [49]	9.7	42.6	21.1	6.9	17.6	5.1	2.5	15.1 \pm 1.5
		ML_Net_with_DS [49]	8.6	35.6	19.6	5.3	15.9	3.2	3.1	13.0 \pm 1.7
		ML_Net_with_RC [49]	8.2	36.9	20.5	4.8	16.2	1.6	0.9	12.7 \pm 1.6
		mi_Net [49]	8.2	28.4	15.1	11.2	15.8	6.8	4.5	12.9 \pm 1.2
		MI-max	0.3	0.1	42.7	4.4	21.9	0.6	13.7	12.0 \pm 0.9
		Polyhedral MI-max	3.1	9.8	33.0	7.4	29.2	0.1	8.5	13.0 \pm 2.2
		MI-max-HL	4.3	6.7	35.7	15.6	24.0	0.1	15.2	14.5 \pm 1.8

performs the other MIL networks on three datasets. Moreover the multiple instance neural network outperforms the multiple instance SVM (mi-SVM and MI-SVM), which can be due to the fact that a linear SVM that are not complex enough.

We can notice that the Maximum Pattern margin methods (mi-SVM and mi_Net) never perform better than the Bag margin ones. This is rather unexpected since those models are designed to better take into account the whole positive bag by assigning an individual label per instance. These models appear to be badly suited for the task of weakly supervised detection in non-photographic databases.

When comparing our MI-max and Polyhedral MI-max models to the baseline MAX and MAXA, we observe that our models consistently perform better. Nevertheless the MAXA model performs well especially on the IconArt or CASPApaintings databases, probably because this model uses all the regions of the negatives images, yielding good discrimination of background regions during inference. The MAX baseline sometimes provides equivalent performances to more complex methods (such as MI-SVM or MI_Net), illustrating the fact that the objectness score (used for selecting candidates in MAX) contains useful information. Also observe that it is faster to train a multiple instance perceptron than several linear SVMs, as is needed for MI-SVM or mi-SVM. This is quantified in Section 4.2.1.

Finally, we observe that both our models MI-max and Polyhedral MI-max provides better results than the others methods on PeopleArt, CASPApaintings, Comic2k, Clipart1k and Watercolor2k datasets.

The dataset IconArt appear to be much more challenging. In this case, our multiple instance methods provide equivalent performances compared to the multiple instance networks. The best performance is obtained by the MI_Net, the MI-max-HL performance being very similar.

4.2.1. Execution Time

One advantage of our method is the relative short time needed for training, as can be seen in Table 8. As can be expected, the SPN and PCL methods are the longest to train due to the fine-tuning of the whole network. Observe

also that the training time for our method MI-max is almost independent of the number of classes and restarts, which is a strong advantage compared to the MI-SVM, mi-SVM, MI_Net and mi_Net models which all need one full training per class and per re-initialization. The SVM based methods are more costly because they don't take advantage of GPU computational power.

Nevertheless, due to the aggregation of several hyperplan with a maximum operator in the Polyhedral MI-max model, we need to do 10 time more epochs than when using MI-max, which explain the strong overload.

Table 8: Execution time of the different models for datasets Watercolor2k and Comic2k, with 1000 images in the training set and 6 visual categories.

Method	Training Duration	Linear to number of class	Linear to number of restarts
No Boxes proposals			
SPN [5]	3000s (20 epochs)	No	•
Selective Search Bounding Boxes proposal			
PCL [76]	6600s	No	•
12000s (13 epochs)			
Faster RCNN Features and boxes proposals	200s		
MAXwith GS	52s	Yes	•
MAXA with GS	2000s	Yes	•
MI-SVM [13]	3000s	Yes	Yes
mi-SVM [13]	30000s	Yes	Yes
MI_Net [49]	1200s (20 epochs)	Yes	Yes
ML_Net_with_DS [49]	1800s (20 epochs)	Yes	Yes
ML_Net_with_RC [49]	1600s (20 epochs)	Yes	Yes
mi_Net [49]	1800s (20 epochs)	Yes	Yes
MI-max	130s (300 epochs)	No	No
Polyhedral MI-max	1100s (3000 epochs)	No	No
MI-max-HL	3000s (300 epochs)	No	Yes

4.3. Fine MI-max models Analysis

In this section we discuss the details of our models and some variations. In particular, we provide an ablation study where we analyze how the choices of a different loss, different set of features and use of the objectness score impact the performances of our models. In Section 4.3.2 a thorough investigation of the main parameters' influence is conducted. From this study we are able to recommend a set of parameters that are suited for our models, thus providing the user with a safe baseline for re-using them. Then, we experimentally show that our method also permits to transfer easily the knowledge between datasets and artistic modalities. In section 4.3.3, we also evaluate the generalization ability of our models across different modalities of images (using classes shared by the different datasets). Finally, in section 4.3.4 some visual results are commented to give an insight on the strengths and shortcomings of our model.

4.3.1. Ablation study

Choice of the loss function : In Table 9, we gather different versions of the two models MI-max and Polyhedral MI-max with two possible modifications. First we replace the *Tanh* based loss in equation (1) by the Hinge loss. Second we suppress the objectness score in the loss function (see section 3.2.2).

The first conclusion that can be drawn is that the use of objectness score significantly increase the performances of our models. This is especially true for the PeopleArt dataset where the performances very strongly decrease without using the objectness score. For the other datasets the performances are always significantly lower without the objectness score. Note that for some classes this drop in detection score is due to the fact that the model detects parts of the

object instead of the whole object when the objectness score is ignored. Such an example can be seen in figure 8 section 4.3.4, where the class for Saint Sebastian is confused with arrows, which is understandable in this case but not desirable. The use of the objectness score often helps avoiding such partial detection cases.

The second conclusion is that replacing the *Tanh* based loss function in equation (1) by a Hinge loss $l(y, \hat{y}) = 1 - \max(0, 1 - y\hat{y})$ generally hinders the performances, except for two cases among the 12 cases of the (dataset,model) possible combinations. In particular the Polyhedral MI-max methods never benefits from a different loss function. This may be due to the fact that, given the difficulty of the task, errors are likely to happen and the *Tanh* function may be more robust and forgiving than the Hing loss which will try hard to correct any errors, especially those with a high negative margin.

Table 9: Mean average precision over the classes of the different datasets (%). Comparison of the proposed MI-max and Polyhedral MI-max methods with different settings. Standard deviation is computed on 10 runs of the method.

Dataset	MI-max				Polyhedral MI-max			
	Main Model	Without score	Hinge loss	Without score and hinge loss	Main Model	Without score	Hinge loss	Without score and hinge loss
PeopleArt	55.5 ± 1.0	0.9 ± 0.4	57.6 ± 1.0	1.7 ± 0.9	58.3 ± 1.2	10.1 ± 3.3	56.6 ± 4.4	18.1 ± 8.6
Watercolor2k	49.5 ± 0.9	32.8 ± 2.2	46.7 ± 1.5	33.8 ± 1.6	46.6 ± 1.3	18.3 ± 4.7	37.5 ± 2.1	24.8 ± 3.3
Clipart1k	38.4 ± 0.8	24.2 ± 1.6	34.8 ± 1.2	22.2 ± 1.8	30.6 ± 0.0	9.6 ± 0.0	16.1 ± 0.0	7.0 ± 0.0
Comic2k	27.0 ± 0.8	17.4 ± 1.5	25.5 ± 1.1	17.3 ± 1.1	24.1 ± 0.0	12.4 ± 0.0	14.2 ± 0.0	11.0 ± 0.0
CASPA paintings	16.2 ± 0.4	18.7 ± 0.8	16.1 ± 0.5	12.6 ± 0.9	14.4 ± 0.0	10.0 ± 0.0	9.4 ± 0.0	3.4 ± 0.0
IconArt	12.0 ± 0.9	6.7 ± 2.5	14.3 ± 2.1	8.2 ± 2.3	13.0 ± 2.2	6.4 ± 2.3	13.3 ± 2.8	8.3 ± 2.0

Features extraction and region proposals choices : We have investigated alternative choices for the Faster RCNN’s features and box proposals : for the boxes we used the unsupervised box proposal algorithm EdgeBoxes [42] and for the features we used a ResNet-152 trained on ImageNet applied to each proposed box. By doing so we must drop the objectness score that is not included in the output of EdgeBoxes.

We can see in Table 10 the performances of the model MI-max (without the objectness score) using those features/boxes compared to the Faster RCNN features/boxes (without objectness score for fair comparison). Regarding the detection task the performances clearly drop when using EdgeBoxes. To further investigate this drop of performance we present in Table 11 the recall score of three box proposals methods (the percentage of ground-truth boxes that are present in the set of all proposed boxes). We can see that EdgeBoxes performs very poorly on a data-set like PeopleArt and never matches the boxes proposed by Faster RCNN.

For the classification task we can see that the MI-max method without objectness score performs honorably in this setting when compared to the use of Faster RCNN’s boxes/features (even slightly better on the IconArt database). This is another proof that bag-level classification (the aim of the training of a MIL algorithm) is not a good proxy for instance-level classification (which is the aim of a detection algorithm). The objectness score can be seen as a very helpful cue to guide the training of a WSOD method. As shown by [79] for classification task, transfer learning of deep models trained for detection tasks is the best way to obtain a detector on new domains even when no bounding

boxes are available.

Table 10: Average precision for detection and classification (%). Two different feature extraction methods are considered in this table (both without objectness score).

Dataset	Metric	Faster RCNN	EdgeBoxes
PeopleArt	AP IuO ≥ 0.5	0.9 \pm 0.4	0.0 \pm 0.0
	Classif AP	92.5 \pm 0.3	92.1 \pm 0.2
Clipart1k	AP IuO ≥ 0.5	24.2 \pm 1.6	3.1 \pm 0.3
	Classif AP	59.4 \pm 1.7	42.8 \pm 1.3
Comic2k	AP IuO ≥ 0.5	17.4 \pm 1.5	1.8 \pm 0.3
	Classif AP	54.9 \pm 2.0	47.9 \pm 1.5
Watercolor2k	AP IuO ≥ 0.5	32.8 \pm 2.2	2.7 \pm 0.5
	Classif AP	78.0 \pm 1.2	71.8 \pm 1.3
CASPA	AP IuO ≥ 0.5	12.6 \pm 0.5	0.3 \pm 0.1
	Classif AP	48.6 \pm 0.6	45.0 \pm 1.2
IconArt	AP IuO ≥ 0.5	6.7 \pm 2.5	5.3 \pm 0.3
	Classif AP	60.4 \pm 1.1	69.2 \pm 0.3

Table 11: Recall (%) at IuO ≥ 0.5 of the boxes proposals for the different methods and databases. Mean over the classes.

Dataset	RPN of Pre-trained Faster RCNN [1]	EdgeBoxes [42]	Selective Search [41]
Number of boxes	300	300	3000-5000
PeopleArt	94.0	15.4	55.7
Clipart1k	91.4	14.4	49.4
Comic2k	82.7	54.1	46.2
Watercolor2k	93.6	61.4	56.8
CASPA	76.6	34.3	51.6
IconArt	75.9	60.0	56.9

4.3.2. Influence of the parameters of the model

In this section, we analyse the influence of the different hyperparameters of our MI-max model. We show in Figure 2 the performances with respect to each of the three following parameters: the number of restarts, the batch size and the regularization term C . We vary one parameter at a time while keeping the others fixed to the already mentioned values (i.e. 11 for the number of restarts, 1000 for the batch size and 1.0 for C).

Although the study in [46] shows that restarts from random points is not always useful for nonconvex models, we find that having about 10 restarts slightly improves the performances and can be taken as a rule of thumb for our models. Notice that the variance of the outcomes is also reduced for such a parameter choice. We also found experimentally that restarts for mi-SVM or MI-SVM reduce the performance in accordance with the experiments in [46]. Then, we observe that increasing the batch size provides better results and often yields a reduction of the variance. For the regularization term, we observe relatively constant performances between 1.0 and 2.0. The value 0.5 seems to be the best for 2 of the datasets (PeopleArt and IconArt, but with a great variance). These experiments also show the necessity of using a regularization term in the loss function.

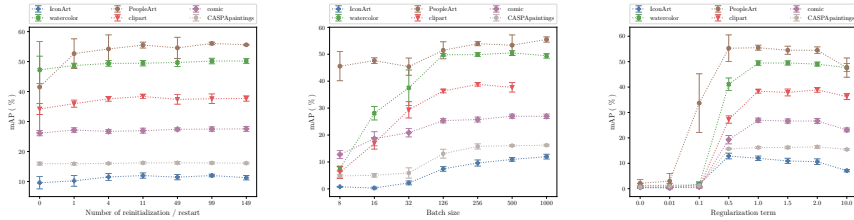


Figure 2: Impact of the different hyperparameters on the MI-max model. Figure must be seen in color.

4.3.3. Cross modalities Knowledge Transfer

Tables tables 12 and 13 present across-domain performance for two our models Polyhedral MI-max and MI-max. We compute the performances of detection for the classes that are shared between the different datasets. Those performances (one run) are compared to the mean performance on the same modality (several runs as before). This experiment illustrates the fact that our method can be transferred to other modality of images. This is sometimes called the "Cross-Depiction Problem" [80] : recognizing visual objects regardless of whether they are painted or depicted in different artistic style.

First, we can see that the Polyhedral MI-max model trained on PeopleArt outperforms the one learned on the target modality for 2 of the 3 datasets (first line). This can be due to the fact the PeopleArt dataset contains many different artistic style. We also observe that the MI-max model badly fails on those three datasets and that the Polyhedral MI-max model generalizes better. Observe also that the fact that the class person is well detected can also be due to the Faster RCNN features that have been trained on a dataset (MS COCO) containing this class.

Finally, we can notice that some datasets such as CASPApaintings and Clipart1k are more challenging that the other maybe due to the difference in the modality for the second one.

This experiment illustrates the fact that our model Polyhedral MI-max generalize well but also that providing a diverse and numerous training set can help to get a better detector trained in a weakly supervised manner.

Table 12: Mean AP (%) at IuO ≥ 0.5 for the common classes between the source and target sets with the MI-max model. In parenthesis the mean performance obtained by learning the detection on the same set (modality).

source set \ target set	PeopleArt	Watercolor2k	Comic2k	Clipart1k	CASPApaintings
PeopleArt	-	0.0 (58.2)	0.0 (37.0)	0.0 (55.5)	-
Watercolor2k	47.4 (55.5)	-	25.8 (27.0)	12.2 (33.4)	15.6 (18.3)
Comic2k	50.4 (55.5)	47.3 (49.5)	-	10.0 (33.4)	15.0 (18.3)
Clipart1k	36.2 (55.5)	44.3 (49.5)	25.2 (27.0)	-	10.8 (14.0)
CASPApaintings	-	33.4 (35.4)	12.2 (15.2)	4.7 (22.5)	-

Table 13: Mean AP (%) at $IuO \geq 0.5$ for the common classes between the source and target sets with the Polyhedral MI-max model. The mean performance obtained by learning the detection on the same set (modality) is displayed between brackets.

source set \ target set	PeopleArt	Watercolor2k	Comic2k	Clipart1k	CASPApaintings
PeopleArt	-	60.0 (59.2)	42.1 (39.5)	54.3 (55.4)	-
Watercolor2k	56.0 (57.3)	-	23.1 (24.1)	11.2 (24.6)	13.8 (18.3)
Comic2k	48.9 (57.3)	42.4 (46.6)	-	7.2 (24.6)	12.5 (18.3)
Clipart1k	52.0 (57.3)	36.7 (46.6)	19.6 (24.1)	-	7.7 (13.6)
CASPApaintings	-	27.5 (39.0)	9.9 (18.1)	4.2 (12.5)	-



Figure 3: One successful example per class using our Polyhedral MI-max detection scheme on Watercolor2k test set. We only show boxes whose scores are over 0.75. Figure must be seen in color.

4.3.4. Visual results from the Polyhedral MI-max model.

In order to give some intuitive insight on the ability of the proposed method, we show some visual illustrations of the performance of the proposed model Polyhedral MI-max, both in successful and failure cases.

Successful detections : We show successful results on various datasets. In figs. 3 and 4 we show various examples of the visual categories we are able to detect, respectively on Watercolor2k and CASPApainting datasets. On Figure 5, we can see the large stylistic diversity that the model is able to detect for a same class, namely person, on the PeopleArt dataset. On Figure 6, one can see some detections on the challenging IconArt dataset.

Failures examples : We can categorize the failures cases into five main categories:

1. Discriminative elements are detected instead of the whole object : the

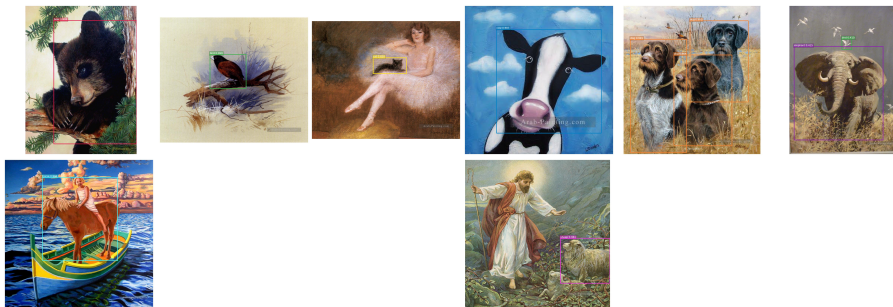


Figure 4: One successful example per class using our Polyhedral MI-max detection scheme on CASPApaintings test set. We only show boxes whose scores are over 0.75, except for the elephant image. Figure must be seen in color.

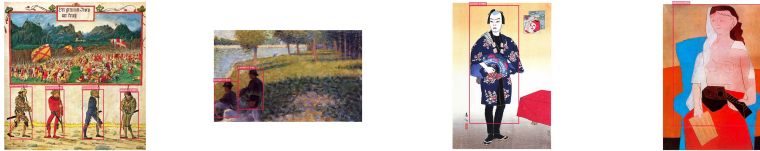


Figure 5: Successful examples using our Polyhedral MI-max detection scheme on PeopleArt test set. One can observe the strong stylistic differences between the images. We only show boxes whose scores are over 0.75. Figure must be seen in color.

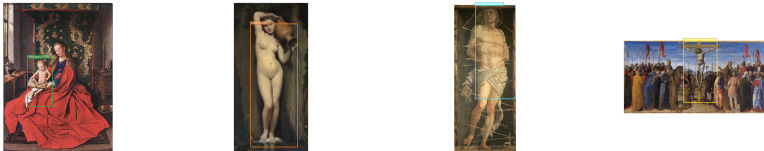


Figure 6: Successful examples of detection of iconographic characters using our Polyhedral MI-max detection scheme on IconArt test set. We only show boxes whose scores are over 0.75. Figure must be seen in color.

hand for instance in Figure 7 for the Polyhedral MI-max without score model or the arrows instead of Saint Sebastian in Figure 8) for the MI-max model without score.

2. Detection of a whole group instead of individual instances (Figure 9).
3. Misclassification of correct bounding box, as in Figure 10.
4. Confusing images (Figure 11, relatively advanced knowledge in art history is needed to know that the child on the left is Saint John the Baptist).

5. Conclusion

In this paper, we confirm that transfer learning of pretrained CNN can provide good model to automatically analyze non photo-realistic images databases. This was previously shown for classification and fully supervised detection tasks, and was here investigated in the case of weakly supervised object detection. We proposed a simple and quick model to solve the multiple instance problem we are

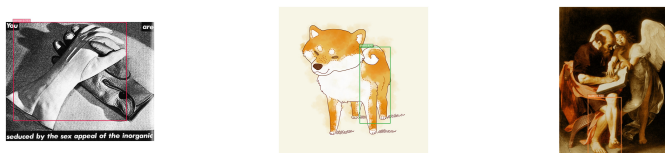


Figure 7: Failure examples using our our Polyhedral MI-max detection scheme on different datasets. We only show boxes whose scores are over 0.75. The most discriminative boxes correspond to parts of the whole objects. On the first image, the gloves are detected instead of a person. On the second one, the back legs and tail are detected as a dog. On the last one, the legs are detected as nudity. Figure must be seen in color.



Figure 8: An example of wrongly detected object at test time, when using MI-max without or with the objectness score. In the first case, arrows or spike are detected instead of Saint Sebastian. Figure must be seen in color.



Figure 9: Failure examples using our our Polyhedral MI-max detection scheme on different datasets. We only show boxes whose scores are over 0.75. Whole groups are detected instead of the instances. Figure must be seen in color.

facing. In future works, we plan to add some constraint in the polyhedral case to force the hyperplanes to be as distinct as possible to get better boundaries, to develop on piece-wise linear model. It might be beneficial to take in more than one instance per bag to learn better detector and catch multi-modal visual category. A more extensive investigation of the different possible features extractor and boxes proposals algorithms could show the flexibility of our model. Another exciting direction is to investigate the potential of weakly supervised learning on large databases with only image-level annotations. For instance, this framework could be used to develop versatile search engine for diverse modalities of images, avoiding the time consuming annotation task. Moreover, we plan to supervise the training of weak detector with a fully-trained classifier in order to remove some obvious mis-classified box candidate as it can be done in classical WSOD method [32]. This could help to provide better detection performances.

Acknowledgements. This work is supported by the "IDI 2017" project funded by the IDEX Paris-Saclay, ANR-11-IDEX-0003-02.



Figure 10: Failure examples using our our Polyhedral MI-max detection scheme on different datasets. We only show boxes whose scores are over 0.75. Mis-classified boxes : on the first image the bird is classified as a dog and on the second one the dog is detected as a cat. Figure must be seen in color.



Figure 11: Failure examples using our our Polyhedral MI-max detection scheme on different datasets. We only show boxes whose scores are over 0.75. Those are confusing images. In the first one a bear in an human posture is detected as a person. In the middle, the horse, the man and other animals are deformed. The last one is a confusing case between Saint John the Baptist and Jesus children who are visually similar. Figure must be seen in color.

References

References

- [1] S. Ren, K. He, R. Girshick, J. Sun, Faster R-CNN: Towards Real-Time Object Detection with Region Proposal Networks, *Advances in neural information processing systems* (2015) 91–99ArXiv: 1506.01497. URL <http://arxiv.org/abs/1506.01497>
- [2] H. Su, J. Deng, L. Fei-Fei, Crowdsourcing Annotations for Visual Object Detection, in: *Workshops at the Twenty-Sixth AAAI Conference on Artificial Intelligence*, 2016, p. 7.
- [3] P. Tubaro, A. A. Casilli, Micro-work, artificial intelligence and the automotive industry, *Journal of Industrial and Business Economics* 46 (3) (2019) 333–345. doi:10.1007/s40812-019-00121-1. URL <http://link.springer.com/10.1007/s40812-019-00121-1>
- [4] H. Bilen, A. Vedaldi, Weakly Supervised Deep Detection Networks, in: *Proceedings of the IEEE Conference on Computer Vision and Pattern Recognition*, IEEE, 2016, pp. 2846–2854. doi:10.1109/CVPR.2016.311. URL <http://ieeexplore.ieee.org/document/7780680/>
- [5] Y. Zhu, Y. Zhou, Q. Ye, Q. Qiu, J. Jiao, Soft Proposal Networks for Weakly Supervised Object Localization, in: *2017 IEEE International Conference on Computer Vision (ICCV)*, 2017, pp. 1859–1868. doi:10.1109/ICCV.2017.204.
- [6] P. Tang, X. Wang, A. Wang, Y. Yan, W. Liu, J. Huang, A. Yuille, Weakly Supervised Region Proposal Network and Object Detection, *Proceedings of the European Conference on Computer Vision (ECCV)* (2018) 352–368.
- [7] T.-H. Vu, H. Jain, M. Bucher, M. Cord, P. Perez, ADVENT: Adversarial Entropy Minimization for Domain Adaptation in Semantic Segmentation, 2019, pp. 2517–2526. URL http://openaccess.thecvf.com/content_CVPR_2019/html/Vu.ADVENT_Adversarial_Entropy_Minimization_for_Domain_Adaptation_in_Semantic_Segmentation_CVPR_2019_paper.html

- [8] J. Yang, N. C. Dvornek, F. Zhang, J. Chapiro, M. Lin, J. S. Duncan, Unsupervised Domain Adaptation via Disentangled Representations: Application to Cross-Modality Liver Segmentation, in: D. Shen, T. Liu, T. M. Peters, L. H. Staib, C. Essert, S. Zhou, P.-T. Yap, A. Khan (Eds.), *Medical Image Computing and Computer Assisted Intervention MICCAI 2019, Lecture Notes in Computer Science*, Springer International Publishing, Cham, 2019, pp. 255–263. doi:10.1007/978-3-030-32245-8_29.
- [9] Y. Li, N. Wang, J. Shi, X. Hou, J. Liu, Adaptive Batch Normalization for practical domain adaptation, *Pattern Recognition* 80 (2018) 109–117. doi:10.1016/j.patcog.2018.03.005.
URL <http://www.sciencedirect.com/science/article/pii/S003132031830092X>
- [10] K. Saenko, B. Kulis, M. Fritz, T. Darrell, Adapting Visual Category Models to New Domains, in: K. Daniilidis, P. Maragos, N. Paragios (Eds.), *Computer Vision ECCV 2010, Lecture Notes in Computer Science*, Springer, Berlin, Heidelberg, 2010, pp. 213–226. doi:10.1007/978-3-642-15561-1_16.
- [11] N. Inoue, R. Furuta, T. Yamasaki, K. Aizawa, Cross-Domain Weakly-Supervised Object Detection through Progressive Domain Adaptation, in: *IEEE Conference on Computer Vision and Pattern Recognition (CVPR 2018)*, IEEE, 2018, arXiv: 1803.11365.
URL <http://arxiv.org/abs/1803.11365>
- [12] M. Fu, Z. Xie, W. Li, L. Duan, Deeply Aligned Adaptation for Cross-domain Object Detection, arXiv:2004.02093 [cs]ArXiv: 2004.02093 (Apr. 2020).
URL <http://arxiv.org/abs/2004.02093>
- [13] S. Andrews, I. Tsochantaridis, T. Hofmann, Support vector machines for multiple-instance learning, in: *Advances in neural information processing systems*, 2003, pp. 577–584.
- [14] O. Russakovsky, J. Deng, H. Su, J. Krause, S. Satheesh, S. Ma, Z. Huang, A. Karpathy, A. Khosla, M. Bernstein, A. C. Berg, L. Fei-Fei, ImageNet Large Scale Visual Recognition Challenge, *International Journal of Computer Vision* 115 (3) (2015) 211–252, arXiv: 1409.0575.
URL <http://arxiv.org/abs/1409.0575>
- [15] M. Everingham, L. Van Gool, C. K. I. Williams, A. Zisserman, The PASCAL Visual Object Classes Challenge 2007 (VOC2007) (2007).
URL <http://www.pascal-network.org/challenges/VOC/voc2007/workshop/index.html>
- [16] T.-Y. Lin, M. Maire, S. Belongie, L. Bourdev, R. Girshick, J. Hays, P. Perona, D. Ramanan, C. L. Zitnick, P. Dollr, Microsoft COCO: Common Objects in Context, in: *European conference on computer vision*, Springer,

- 2014, pp. 740–755, arXiv: 1405.0312.
 URL <http://arxiv.org/abs/1405.0312>
- [17] A. Kuznetsova, H. Rom, N. Alldrin, J. Uijlings, I. Krasin, J. Pont-Tuset, S. Kamali, S. Popov, M. Mallocci, A. Kolesnikov, T. Duerig, V. Ferrari, The Open Images Dataset V4, *International Journal of Computer Vision* (Mar. 2020). doi:10.1007/s11263-020-01316-z.
 URL <https://doi.org/10.1007/s11263-020-01316-z>
- [18] e. Zhang, C. Kaeser-Chen, G. Vesom, J. Choi, M. Kessler, S. Belongie, The iMet Collection 2019 Challenge Dataset, arXiv:1906.00901 [cs]ArXiv: 1906.00901 (Jun. 2019).
 URL <http://arxiv.org/abs/1906.00901>
- [19] M. J. Wilber, C. Fang, H. Jin, A. Hertzmann, J. Collomosse, S. Belongie, BAM! The Behance Artistic Media Dataset for Recognition Beyond Photography, in: *IEEE International Conference on Computer Vision (ICCV)*, 2017, pp. 1211–1220, arXiv: 1704.08614.
 URL <http://arxiv.org/abs/1704.08614>
- [20] N. Westlake, H. Cai, P. Hall, Detecting People in Artwork with CNNs, *European Conference on Computer Vision (2016)* 825–841ArXiv: 1610.08871. doi:10.1007/978-3-319-46604-0_57.
 URL <http://arxiv.org/abs/1610.08871>
- [21] B. Seguin, L. Costiner, I. di Lenardo, F. Kaplan, New Techniques for the Digitization of Art Historical Photographic Archives - the Case of the Cini Foundation in Venice, *Archiving Conference 2018 (1)* (2018) 1–5. doi:10.2352/issn.2168-3204.2018.1.0.2.
 URL <http://www.ingentaconnect.com/content/10.2352/issn.2168-3204.2018.1.0.2>
- [22] N. Gonthier, Y. Gousseau, S. Ladjal, O. Bonfait, Weakly Supervised Object Detection in Artworks, in: *Computer Vision ECCV 2018 Workshops, Lecture Notes in Computer Science*, Springer International Publishing, 2018, pp. 692–709.
- [23] T. G. Dietterich, R. H. Lathrop, T. Lozano-Prez, Solving the multiple instance problem with axis-parallel rectangles, *Artificial Intelligence* 89 (1) (1997) 31–71. doi:10.1016/S0004-3702(96)00034-3.
 URL <http://www.sciencedirect.com/science/article/pii/S0004370296000343>
- [24] M. H. Nguyen, L. Torresani, F. de la Torre, C. Rother, Weakly supervised discriminative localization and classification: a joint learning process, in: *2009 IEEE 12th International Conference on Computer Vision*, 2009, pp. 1925–1932, iSSN: 2380-7504. doi:10.1109/ICCV.2009.5459426.

- [25] P. Siva, Tao Xiang, Weakly supervised object detector learning with model drift detection, in: 2011 International Conference on Computer Vision, IEEE, Barcelona, Spain, 2011, pp. 343–350. doi:10.1109/ICCV.2011.6126261.
URL <http://ieeexplore.ieee.org/document/6126261/>
- [26] H. O. Song, R. Girshick, S. Jegelka, J. Mairal, Z. Harchaoui, T. Darrell, On learning to localize objects with minimal supervision, in: Proceedings of the 31st International Conference on Machine Learning, Vol. 32, Beijing, China, 2014, p. 9.
- [27] R. Girshick, J. Donahue, T. Darrell, J. Malik, Rich Feature Hierarchies for Accurate Object Detection and Semantic Segmentation, in: 2014 IEEE Conference on Computer Vision and Pattern Recognition, 2014, pp. 580–587. doi:10.1109/CVPR.2014.81.
- [28] A. Diba, V. Sharma, A. Pazandeh, H. Pirsiavash, L. V. Gool, Weakly Supervised Cascaded Convolutional Networks, in: Proceedings of the IEEE Conference on Computer Vision and Pattern Recognition, IEEE, 2017, pp. 5131–5139. doi:10.1109/CVPR.2017.545.
URL <http://ieeexplore.ieee.org/document/8100028/>
- [29] V. Kantorov, M. Oquab, M. Cho, I. Laptev, ContextLocNet: Context-Aware Deep Network Models for Weakly Supervised Localization, in: European Conference on Computer Vision, Springer, Cham, 2016, pp. 350–365, arXiv: 1609.04331.
URL <http://arxiv.org/abs/1609.04331>
- [30] P. Tang, X. Wang, X. Bai, W. Liu, Multiple Instance Detection Network with Online Instance Classifier Refinement, IEEE, 2017, pp. 3059–3067. doi:10.1109/CVPR.2017.326.
URL <http://ieeexplore.ieee.org/document/8099809/>
- [31] R. Girshick, Fast R-CNN, in: Proceedings of the IEEE international conference on computer vision, 2015, pp. 1440–1448, arXiv: 1504.08083.
URL <http://arxiv.org/abs/1504.08083>
- [32] F. Wan, P. Wei, J. Jiao, Z. Han, Q. Ye, Min-Entropy Latent Model for Weakly Supervised Object Detection, Proceedings of the IEEE Conference on Computer Vision and Pattern Recognition (2018) 1297–1306.
- [33] X. Zhang, J. Feng, H. Xiong, Q. Tian, Zigzag Learning for Weakly Supervised Object Detection, in: CVPR, 2018, pp. 4262–4270, arXiv: 1804.09466.
URL <http://arxiv.org/abs/1804.09466>
- [34] Y. Zhang, Y. Bai, M. Ding, Y. Li, B. Ghanem, W2F: A Weakly-Supervised to Fully-Supervised Framework for Object Detection, in: Proceedings of the IEEE Conference on Computer Vision and Pattern Recognition, 2018, pp. 928–936.

- [35] X. Dong, D. Meng, F. Ma, Y. Yang, A Dual-Network Progressive Approach to Weakly Supervised Object Detection, in: Proceedings of the 25th ACM International Conference on Multimedia, MM '17, ACM, New York, NY, USA, 2017, pp. 279–287. doi:10.1145/3123266.3123455.
URL <http://doi.acm.org/10.1145/3123266.3123455>
- [36] F. Wan, C. Liu, W. Ke, X. Ji, J. Jiao, Q. Ye, C-MIL: Continuation Multiple Instance Learning for Weakly Supervised Object Detection, CVPRArXiv: 1904.05647 (Apr. 2019).
URL <http://arxiv.org/abs/1904.05647>
- [37] Y. Tang, X. Wang, E. Dellandrea, L. Chen, Weakly Supervised Learning of Deformable Part-Based Models for Object Detection via Region Proposals, IEEE Transactions on Multimedia 19 (2) (2017) 393–407. doi:10.1109/TMM.2016.2614862.
URL <http://ieeexplore.ieee.org/document/7581027/>
- [38] D. Li, J.-B. Huang, Y. Li, S. Wang, M.-H. Yang, Weakly Supervised Object Localization with Progressive Domain Adaptation, in: Proceedings of the IEEE Conference on Computer Vision and Pattern Recognition, IEEE, 2016, pp. 3512–3520. doi:10.1109/CVPR.2016.382.
URL <http://ieeexplore.ieee.org/document/7780751/>
- [39] A. Arun, C. V. Jawahar, M. P. Kumar, Dissimilarity Coefficient based Weakly Supervised Object Detection, CVPRArXiv: 1811.10016 (2019).
URL <http://arxiv.org/abs/1811.10016>
- [40] M. Oquab, L. Bottou, I. Laptev, J. Sivic, Is object localization for free? - Weakly-supervised learning with convolutional neural networks, in: Proceedings of the IEEE Conference on Computer Vision and Pattern Recognition, 2015, pp. 685–694.
URL http://www.cv-foundation.org/openaccess/content_cvpr_2015/html/Oquab_Is_Object_Localization_2015_CVPR_paper.html
- [41] J. R. R. Uijlings, K. E. A. van de Sande, T. Gevers, A. W. M. Smeulders, Selective Search for Object Recognition, International Journal of Computer Vision 104 (2) (2013) 154–171. doi:10.1007/s11263-013-0620-5.
URL <http://link.springer.com/10.1007/s11263-013-0620-5>
- [42] C. L. Zitnick, P. Dollr, Edge Boxes: Locating Object Proposals from Edges, in: Computer Vision ECCV 2014, Vol. 8693, Springer International Publishing, Cham, 2014, pp. 391–405. doi:10.1007/978-3-319-10602-1_26.
URL http://link.springer.com/10.1007/978-3-319-10602-1_26
- [43] P. F. Felzenszwalb, R. B. Girshick, D. McAllester, D. Ramanan, Object Detection with Discriminatively Trained Part-Based Models, IEEE Transactions on Pattern Analysis and Machine Intelligence 32 (9) (2010) 1627–1645. doi:10.1109/TPAMI.2009.167.

- [44] P. V. Gehler, O. Chapelle, Deterministic Annealing for Multiple-Instance Learning, in: Artificial Intelligence and Statistics, 2007, pp. 123–130.
URL <http://proceedings.mlr.press/v2/gehler07a.html>
- [45] A. Joulin, F. Bach, A convex relaxation for weakly supervised classifiers, in: ICML, 2012, p. 8.
- [46] G. Doran, S. Ray, A theoretical and empirical analysis of support vector machine methods for multiple-instance classification, Machine Learning 97 (1-2) (2014) 79–102. doi:10.1007/s10994-013-5429-5.
URL <http://link.springer.com/10.1007/s10994-013-5429-5>
- [47] J. Ramon, L. D. Raedt, Multi Instance Neural Networks, Proceedigs of ICML (2000).
- [48] Z.-H. Zhou, M.-L. Zhang, Neural Networks for Multi-Instance Learning, in: Proceedings of the International Conference on Intelligent Information Technology, Beijing, China, 2002, p. 14.
- [49] X. Wang, Y. Yan, P. Tang, X. Bai, W. Liu, Revisiting Multiple Instance Neural Networks, Pattern Recognition 74 (2018) 15–24, arXiv: 1610.02501.
URL <http://arxiv.org/abs/1610.02501>
- [50] M.-A. Carbonneau, V. Cheplygina, E. Granger, G. Gagnon, Multiple Instance Learning: A Survey of Problem Characteristics and Applications, Pattern Recognition 77 (2016) 329–353, arXiv: 1612.03365. doi: 10.1016/j.patcog.2017.10.009.
URL <http://arxiv.org/abs/1612.03365>
- [51] M.-A. Carbonneau, E. Granger, A. J. Raymond, G. Gagnon, Robust multiple-instance learning ensembles using random subspace instance selection, Pattern Recognition 58 (2016) 83–99. doi:10.1016/j.patcog.2016.03.035.
URL <https://linkinghub.elsevier.com/retrieve/pii/S0031320316300346>
- [52] E. J. Crowley, A. Zisserman, In search of art, in: Workshop at the European Conference on Computer Vision, Springer, 2014, pp. 54–70.
URL http://link.springer.com/chapter/10.1007/978-3-319-16178-5_4
- [53] E. J. Crowley, Visual Recognition in Art using Machine Learning, Ph.D. thesis, University of Oxford (2016).
URL <http://www.robots.ox.ac.uk/~vgg/publications/2016/Crowley16a/crowley16a.pdf>
- [54] R. Yin, E. Monson, E. Honig, I. Daubechies, M. Maggioni, Object recognition in art drawings: Transfer of a neural network, in: 2016 IEEE International Conference on Acoustics, Speech and Signal Processing (ICASSP), IEEE, Shanghai, 2016, pp. 2299–2303. doi:10.1109/ICASSP.2016.7472087.
URL <http://ieeexplore.ieee.org/document/7472087/>

- [55] G. Strezoski, M. Worning, OmniArt: A Large-scale Artistic Benchmark, *ACM Transactions on Multimedia Computing, Communications, and Applications (TOMM) - Special Section on Deep Learning for Intelligent Multimedia Analytics* 14 (4) (2018). doi:10.1145/3273022.
- [56] A. Lecoutre, B. Negrevergne, F. Yger, Recognizing Art Style Automatically in painting with deep learning, in: *Asian conference on machine learning, JMLR: Workshop and Conference Proceedings*, 2017, pp. 327–342.
- [57] H. Mao, M. Cheung, J. She, DeepArt : Learning Joint Representations of Visual Arts, in: *Proceedings of the 2017 ACM on Multimedia Conference*, ACM Press, 2017, pp. 1183–1191. doi:10.1145/3123266.3123405.
URL <http://dl.acm.org/citation.cfm?doid=3123266.3123405>
- [58] A. Elgammal, M. Mazzone, B. Liu, D. Kim, M. Elhoseiny, The Shape of Art History in the Eyes of the Machine, in: *Thirty-Second AAAI Conference on Artificial Intelligence.*, 2018, arXiv: 1801.07729.
URL <http://arxiv.org/abs/1801.07729>
- [59] M. Sabatelli, M. Kestemont, W. Daelemans, P. Geurts, Deep Transfer Learning for Art Classification Problems, in: *ECCV*, Munich, 2018, p. 17.
- [60] C. Florea, Mihai Badea, Laura Florea, Constantin Vertan, Domain Transfer for Delving into Deep Networks Capacity to De-Abstract Art, in: *Scandinavian Conference on Image Analysis*, Vol. 10269 of *Lecture Notes in Computer Science*, Springer, Cham, 2017, pp. 337–349. doi:10.1007/978-3-319-59126-1.
URL <http://link.springer.com/10.1007/978-3-319-59126-1>
- [61] N. van Noord, E. Postma, Learning scale-variant and scale-invariant features for deep image classification, *Pattern Recognition* 61 (2017) 583–592. doi:10.1016/j.patcog.2016.06.005.
URL <http://linkinghub.elsevier.com/retrieve/pii/S0031320316301224>
- [62] B. Seguin, Striolo Carlotta, Isabella diLenardo, Kaplan Frederic, Visual Link Retrieval in a Database of Paintings, *Computer Vision ECCV 2016 Workshops* (2016). doi:978-3-319-46604-0_52.
URL <https://infoscience.epfl.ch/record/223771/files/Seguin%20et%20al.%20-%202016%20-%20Visual%20Link%20Retrieval%20in%20a%20Database%20of%20Paintings.pdf>
- [63] T. Jenicek, O. Chum, Linking Art through Human Poses, arXiv:1907.03537 [cs]ArXiv: 1907.03537 (Jul. 2019).
URL <http://arxiv.org/abs/1907.03537>
- [64] P. Bongini, F. Becattini, A. D. Bagdanov, A. Del Bimbo, Visual Question Answering for Cultural Heritage, arXiv:2003.09853 [cs]ArXiv: 2003.09853 (Mar. 2020).
URL <http://arxiv.org/abs/2003.09853>

- [65] X. Shen, A. A. Efros, M. Aubry, Discovering Visual Patterns in Art Collections with Spatially-consistent Feature Learning, in: Proceedings of the IEEE Conference on Computer Vision and Pattern Recognition, 2019, arXiv: 1903.02678.
URL <http://arxiv.org/abs/1903.02678>
- [66] R. Del Chiaro, A. D. Bagdanov, A. Del Bimbo, Webly-supervised Zero-shot Learning for Artwork Instance Recognition, Pattern Recognition Letters (Oct. 2019). doi:10.1016/j.patrec.2019.09.027.
URL <http://www.sciencedirect.com/science/article/pii/S0167865519302739>
- [67] N. Garcia, B. Renoust, Y. Nakashima, Context-Aware Embeddings for Automatic Art Analysis, Proceedings of the 2019 on International Conference on Multimedia Retrieval (2019) 25–33ArXiv: 1904.04985. doi: 10.1145/3323873.3325028.
URL <http://arxiv.org/abs/1904.04985>
- [68] S. Bianco, D. Mazzini, P. Napoletano, R. Schettini, Multitask Painting Categorization by Deep Multibranch Neural Network, Expert Systems with Applications 135 (2019) 90–101, arXiv: 1812.08052. doi:https://doi.org/10.1016/j.eswa.2019.05.036.
URL <http://www.sciencedirect.com/science/article/pii/S0957417419303720>
- [69] M. Fiorucci, M. Khoroshiltseva, M. Pontil, A. Traviglia, A. Del Bue, S. James, Machine Learning for Cultural Heritage: A Survey, Pattern Recognition Letters (Feb. 2020). doi:10.1016/j.patrec.2020.02.017.
URL <http://www.sciencedirect.com/science/article/pii/S0167865520300532>
- [70] K. Saito, Y. Ushiku, T. Harada, K. Saenko, Strong-Weak Distribution Alignment for Adaptive Object Detection, CVPR 2019ArXiv: 1812.04798 (Apr. 2019).
URL <http://arxiv.org/abs/1812.04798>
- [71] D. Li, Y. Yang, Y.-Z. Song, T. M. Hospedales, Deeper, Broader and Artier Domain Generalization, in: ICCV, 2017, arXiv: 1710.03077.
URL <http://arxiv.org/abs/1710.03077>
- [72] C. Thomas, A. Kovashka, Artistic Object Recognition by Unsupervised Style Adaptation, in: Asian Conference on Computer Vision, Springer, Cham, 2018, pp. 460–476, arXiv: 1812.11139.
URL <http://arxiv.org/abs/1812.11139>
- [73] S. Lang, N. Ufer, B. Ommer, Finding Visual Patterns in Artworks: An Interactive Search Engine to Detect Objects in Artistic Images, in: DH, 2019.
URL <https://dev.clariah.nl/files/dh2019/boa/0721.html>

- [74] F. Rosenblatt, The Perceptron: A Probabilistic Model for Information Storage and Organization, *Psychological Review* 65 (6) (1958) 386–408.
- [75] N. Megiddo, On the complexity of polyhedral separability, *Discrete & Computational Geometry* 3 (4) (1988) 325–337. doi:10.1007/BF02187916.
URL <http://link.springer.com/10.1007/BF02187916>
- [76] P. Tang, X. Wang, S. Bai, W. Shen, X. Bai, W. Liu, A. Yuille, PCL: Proposal Cluster Learning for Weakly Supervised Object Detection, *IEEE transactions on pattern analysis and machine intelligence* ArXiv: 1807.03342 (2018).
URL <http://arxiv.org/abs/1807.03342>
- [77] S. Kornblith, J. Shlens, Q. V. Le, Do Better ImageNet Models Transfer Better ?, *Proceedings of the IEEE conference on computer vision and pattern recognition* (2018) 2661–2671 ArXiv: 1805.08974.
URL <http://arxiv.org/abs/1805.08974>
- [78] E. J. Crowley, A. Zisserman, The Art of Detection, in: *European Conference on Computer Vision*, Springer, 2016, pp. 721–737.
URL http://link.springer.com/chapter/10.1007/978-3-319-46604-0_50
- [79] J. Donahue, Y. Jia, O. Vinyals, J. Hoffman, N. Zhang, E. Tzeng, T. Darrell, DeCAF: A Deep Convolutional Activation Feature for Generic Visual Recognition, in: *International conference on machine learning*, 2014, pp. 647–655, arXiv: 1310.1531.
URL <http://arxiv.org/abs/1310.1531>
- [80] P. Hall, H. Cai, Q. Wu, T. Corradi, Cross-depiction problem: Recognition and synthesis of photographs and artwork, *Computational Visual Media* 1 (2) (2015) 91–103. doi:10.1007/s41095-015-0017-1.
URL <http://link.springer.com/10.1007/s41095-015-0017-1>